

## Inhibition of IGF-1 receptor enhances eribulin-induced DNA damage in colorectal cancer

吉弘, 知恭

<https://hdl.handle.net/2324/7363621>


---

出版情報 : Kyushu University, 2024, 博士 (医学), 課程博士  
バージョン :

権利関係 : © 2022 The Authors. Cancer Science published by John Wiley & Sons Australia, Ltd on behalf of Japanese Cancer Association.



# Inhibition of insulin-like growth factor-1 receptor enhances eribulin-induced DNA damage in colorectal cancer

Tomoyasu Yoshihiro<sup>1</sup> | Hiroshi Ariyama<sup>2</sup>  | Kyoko Yamaguchi<sup>2</sup> | Takashi Imajima<sup>1</sup> | Satoru Yamaga<sup>1</sup> | Kenji Tsuchihashi<sup>2</sup> | Taichi Isobe<sup>3</sup>  | Hitoshi Kusaba<sup>1</sup> | Koichi Akashi<sup>1</sup> | Eishi Baba<sup>3</sup> 

<sup>1</sup>Department of Medicine and Biosystemic Science, Kyushu University Graduate School of Medical Sciences, Fukuoka, Japan

<sup>2</sup>Department of Hematology, Oncology and Cardiovascular Medicine, Kyushu University Hospital, Fukuoka, Japan

<sup>3</sup>Department of Oncology and Social Medicine, Graduate School of Medical Sciences, Kyushu University, Fukuoka, Japan

## Correspondence

Eishi Baba, Department of Oncology and Social Medicine, Graduate School of Medical Sciences, Kyushu University, 3-1-1 Maidashi, Higashi-ku, Fukuoka 812-8582, Japan.

Email: [baba.eishi.889@m.kyushu-u.ac.jp](mailto:baba.eishi.889@m.kyushu-u.ac.jp)

## Funding information

Shinnihon Foundation of Advanced Medical Treatment Research

## Abstract

Microtubule targeting agents (MTAs) such as taxanes are broadly used for the treatment of patients with cancer. Although MTAs are not effective for treatment of colorectal cancer (CRC), preclinical studies suggest that a subset of patients with CRC, especially those with cancers harboring the *BRAF* mutation, could benefit from such agents. However, two MTAs, eribulin (Eri) and vinorelbine, have shown limited clinical efficacy. Here, we report that insulin-like growth factor 1 receptor (IGF-1R) signaling is involved in Eri resistance. Using CRC cell lines, we showed that Eri induces activation and subsequent translocation of IGF-1R to the nucleus. When the activation and/or nuclear translocation of IGF-1R was inhibited, Eri induced DNA damage and enhanced G<sub>2</sub>/M arrest. In a xenograft model using the Eri-resistant SW480 cell line, the combination of Eri and the IGF-1R inhibitor linsitinib suppressed tumor growth more efficiently than either single agent. Thus, our results indicated that combination dosing with Eri and an IGF-1R inhibitor could overcome Eri resistance and offer a therapeutic opportunity in CRC.

## KEYWORDS

colorectal cancer, eribulin, IGF-1R, microtubule, ROS

## 1 | INTRODUCTION

Microtubules function as key components of intracellular transport, cell migration, and mitosis. Microtubule targeting agents (MTAs) such as taxanes show antitumor activity by disrupting tubulin dynamics, resulting in G<sub>2</sub>/M phase cell cycle arrest and subsequent apoptosis. To date, MTAs have been used widely for treatment of breast, prostate, and lung cancers, diseases that rank first to third as the most common causes of cancer deaths in the world.<sup>1</sup> For colorectal cancer (CRC), which is the fourth most

common cause of cancer deaths, MTAs show limited efficacy and have not been used clinically. Recently, preclinical research has suggested that *BRAF*-mutated CRC is vulnerable to MTAs,<sup>2</sup> encouraging researchers to undertake two phase II studies using either vinorelbine<sup>3</sup> or eribulin (Eri),<sup>4</sup> two compounds of this class. Unfortunately, both studies reported disappointing results, suggesting further research is needed to improve treatment outcomes for the use of MTAs in patients with CRC, including the identification of predictive biomarkers or efficacious combination therapies.

This is an open access article under the terms of the [Creative Commons Attribution-NonCommercial](https://creativecommons.org/licenses/by-nc/4.0/) License, which permits use, distribution and reproduction in any medium, provided the original work is properly cited and is not used for commercial purposes.

© 2022 The Authors. *Cancer Science* published by John Wiley & Sons Australia, Ltd on behalf of Japanese Cancer Association.

Insulin-like growth factor 1 receptor (IGF-1R) is a receptor tyrosine kinase (RTK) that is known as a key mediator of energy metabolism and growth. Like other RTKs, such as epidermal growth factor receptor (EGFR) and human epidermal growth factor receptor 2 (HER2), IGF-1R is overexpressed in cancers, contributing to unregulated growth.<sup>5</sup> In breast and ovarian cancer, IGF-1R signaling confers MTA resistance,<sup>6,7</sup> but the precise mechanism whereby IGF-1R contributes to such resistance remains elusive. In addition to IGF-1R's activation of well-described downstream signaling pathways involving PI3K/Akt and MAPK, IGF-1R at the cell surface has been reported to be transported to the nucleus following clathrin-dependent endocytosis; this translocation is involved in cancer progression.<sup>8</sup> Nuclear localization of IGF-1R increases cyclin D1 expression and promotes cell proliferation, and is involved in DNA damage tolerance by mediating proliferating cell nuclear antigen ubiquitination upon external DNA damage.<sup>9,10</sup> Furthermore, nuclear translocation of IGF-1R has been reported to contribute to resistance to gefitinib, an inhibitor of the EGFR tyrosine kinase, indicating IGF-1R's important role in cancer biology.<sup>11</sup>

The antitumor activity of chemotherapeutic compounds such as platinum drugs and topoisomerase inhibitors relies on the induction of DNA damage.<sup>12</sup> Reactive oxygen species (ROS) are a key mediator of DNA damage; recent studies have shown that ROS increasingly accumulate during G<sub>2</sub>/M arrest.<sup>13</sup> Although the main mechanism of action of MTAs is induction of mitotic arrest, prolonged mitotic arrest can lead to DNA damage.<sup>14</sup> Thus, we hypothesized that MTAs can cause ROS-induced DNA damage, and that nuclear localization of IGF-1R mediates MTA resistance by ameliorating this DNA damage.

In the present study, we explored the mechanism of resistance to Eri using CRC cell lines. We revealed that activation and subsequent nuclear translocation of IGF-1R was observed after exposure of CRC cells to Eri. Impeding IGF-1R signaling, either by use of an RTK inhibitor or by preventing nuclear translocation of IGF-1R, potentiated Eri-induced G<sub>2</sub>/M phase arrest and DNA damage, leading to the eradication of Eri-resistant cells both in vitro and in vivo.

## 2 | MATERIALS AND METHODS

### 2.1 | Cell culture and chemicals

Colorectal cancer cell lines (colo205, HCT116, HT29, SW480, and DLD1) were obtained from ATCC and colo320 was provided by Riken BRC through the National BioResource Project, Japan. The detail of cell culture and chemicals are shown in Document S1.

### 2.2 | Cell viability assay

Cell viability was assessed by the WST-8 assay using CCK-8 (Dojindo Laboratories) according to the manufacturer's instructions. The percentage of cell viability relative to the vehicle-treated controls was determined.

### 2.3 | Cell cycle analysis

The detailed protocols are shown in Appendix S1.

### 2.4 | Immunocytochemistry

The detailed protocols are shown in Appendix S1. Primary Abs used are listed in Table S1.

### 2.5 | Western blot analysis

The detailed protocols are shown in Appendix S1. Primary Abs used are listed in Table S1.

### 2.6 | Evaluation of ROS production

Cells were seeded in glass-bottom dishes and then incubated with test agents for 24 h. A ROS assay kit – Highly Sensitive DCFH-DA (dichloro-dihydro-fluorescein diacetate) (Dojindo Laboratories) was used according to the manufacturer's instructions.

### 2.7 | Generation of KO cell lines using the CRISPR/Cas9 system

To establish KO cell lines, we cloned single guide RNAs (sgRNAs) into LentiGuide-Puro (#52963; Addgene). The sgRNA sequences were selected from the list provided in the GeCKO version 2 human gRNA library<sup>15</sup>; sequences used in this study are shown in Table S2. LentiCas9-Blast (#52962; Addgene), encoding both the *Streptococcus pyogenes* Cas9 protein and a blasticidin resistance protein, was used for Cas9 expression. LentiGuide-Puro and LentiCas9-Blast were gifts from Feng Zhang (Addgene plasmid #52963; <http://n2t.net/addgene:52963>; RRID: Addgene\_52,963, Addgene plasmid #52962; <http://n2t.net/addgene:52962>; RRID: Addgene\_52,962).<sup>15</sup> To produce lentiviral particles, HEK293T cells cultured in DMEM (Fujifilm Wako Pure Chemical Corporation) supplemented with 10% heat-inactivated FBS and 1% penicillin–streptomycin were transfected with 6.0 µg psPAX2 (#12260; Addgene), 4.1 µg VSV.G (#14888; Addgene), and 10 µg lentiviral vector using linear polyethylenimine (Polysciences). The psPAX2 and VSV.G vectors were gifts from Didier Trono (Addgene; <http://n2t.net/addgene:12260>; RRID: Addgene\_12,260) and Tannishtha Reya (Addgene; <http://n2t.net/addgene:14888>; RRID: Addgene\_14,888), respectively.<sup>16</sup> Medium was changed 6 h after transfection and lentiviral supernatants were collected at 48 and 72 h posttransfection; the supernatants were then concentrated by ultracentrifugation (100,000g for 2 h at 4°C with a Hitachi CS100FNX S50A-2254 rotor). The detailed protocols of lentivirus transduction are shown in Appendix S1.

## 2.8 | In vivo experiment

NOD.Cg-Prkdc<sup>scid</sup>Il2rg<sup>tm1Wjl</sup>/SzJ (NSG) mice were purchased from Charles River Laboratories. SW480 cells ( $1 \times 10^6$ /mouse) were injected subcutaneously in the right flank of each animal. After the mean tumor diameter reached 5 mm, treatment with Eri and/or linsitinib (LINSI) was initiated. Eribulin was administered at 0.25 mg/kg, once per week, by intravenous injection into the lateral tail vein; LINSI was administered at 50 mg/kg, once daily, by oral gavage. Body weight and tumor width and length were measured once every 3 days. Tumor volume was calculated by the formula for volume of an ellipsoid sphere (volume = width<sup>2</sup> × length/2). The animal study protocol was approved by the Ethics Committee of Kyushu University (Approval No. A-21-227-0).

## 2.9 | Immunohistochemistry

The detailed protocols are shown in Appendix S1. Primary Abs used are listed in Table S1.

## 2.10 | Statistical analysis

All statistical analyses were carried out using JMP software (SAS Institute Japan). Differences between groups were analyzed by two-tailed one-way ANOVA with post hoc Tukey–Kramer tests where indicated. Values of  $p < 0.05$  were considered statistically significant.

# 3 | RESULTS

## 3.1 | Analysis of Eri sensitivity and mechanism of action in CRC cell lines

To investigate whether Eri shows antitumor effects against CRC cells, we used the WST-8 assay and quantified cell viability after 72 h of Eri exposure. Although significant growth inhibition was observed in colo205 and HCT116 cells at 1 nM, other CRC cell lines were relatively resistant to Eri, showing IC<sub>50</sub> values of greater than 10 nM (Figure 1A). As for BRAF mutation status, colo205 (known to harbor a BRAF mutation) was sensitive to Eri, whereas HT29 (also known to harbor a BRAF mutation) was resistant to Eri.

Eribulin has been reported to exert antitumor effects by inhibiting tubulin dynamics and inducing G<sub>2</sub>/M arrest. Therefore, cell cycle analysis was carried out by flow cytometry to confirm whether the same mechanism of action applied against CRC cells. Increases of tetraploid DNA content and sub-G<sub>1</sub> peaks, indicating profound G<sub>2</sub>/M arrest and apoptosis, respectively, were observed after 24 h of exposure of the Eri-sensitive line HCT116 to Eri at concentrations of 5 nM or more (Figure 1B). In contrast, the Eri-resistant line SW480 showed only a slight increase in the proportion of G<sub>2</sub>/M-arrested cells, even with exposure at 20 nM Eri.

To confirm whether Eri exposure disturbed tubulin dynamics in HCT116 cells, we undertook immunofluorescent staining of  $\beta$ -tubulin and  $\gamma$ -tubulin. Exposure of HCT116 to 5 nM Eri for 24 h resulted in the formation of abnormal mitotic spindles, as detected by  $\beta$ -tubulin staining, and to the formation of multipolar spindles, as detected by  $\gamma$ -tubulin staining (Figure 1C); both observations suggested disturbance of tubulin dynamics following Eri exposure.

These findings showed that Eri induces G<sub>2</sub>/M arrest and subsequent apoptosis by disrupting tubulin dynamics in an Eri-sensitive CRC cell line. Moreover, BRAF mutation status did not appear to be a predictive biomarker for Eri sensitivity.

## 3.2 | Activation of IGF-1R/insulin receptor pathway confers Eri resistance

Some CRC cells are resistant to Eri, as shown in Figure 1; therefore, we next sought to explore the mechanism of resistance to this MTA in these lines. Given that the IGF signaling pathway has been reported to be involved in resistance to other MTAs,<sup>6,7</sup> we assessed the effect of Eri treatment on IGF-1R/insulin receptor (INSR) activation in the Eri-resistant SW480 line by western blotting. Exposure to Eri results in increased accumulation of phosphorylated IGF-1R/INSR and its downstream effector Akt, indicating activation of IGF signaling upon Eri exposure (Figure 2A). In contrast, the Eri-sensitive HCT116 cell line showed lower accumulation of IGF-1R/INSR compared to SW480, and no apparent change in IGF-1R/INSR activation compared to baseline in HCT116.

Based on these results, we next investigated whether inhibition of IGF signaling disrupts Eri resistance; specifically, we used LINSI and NVP-AEW541 (AEW), small molecule inhibitors of the IGF-1R/INSR tyrosine kinase. Although LINSI (at 5  $\mu$ M) and AEW (at 500 nM) alone provided slight growth suppression of SW480 cells, each enhanced Eri's antitumor activity when combined with Eri (Figure 2B). To elucidate the mechanism whereby Eri plus an IGF-1R/INSR inhibitor causes cytotoxicity, we undertook cell cycle analysis by flow cytometry. As shown in Figure 2C, combination treatment induced apparent G<sub>2</sub>/M arrest and subsequent apoptosis compared to Eri alone, yielding a cell cycle pattern that resembled that of HCT116 cells treated with Eri alone.

To validate the efficacy of the combination of Eri and IGF-1R inhibition, we utilized other Eri resistant cell lines, HT29 and colo320. As shown in Figures S1 and S2, combination treatment suppressed cell growth more significantly and induced profound G<sub>2</sub>/M arrest, which was similar to what was observed in SW480 cells. These results suggested that the combination of Eri and IGF-1R inhibitor showed promising antiproliferative activity irrespective of RAS or BRAF mutation status.

To verify the results of the cell cycle analysis, expression of cell cycle- and apoptosis-related proteins was analyzed using western blotting. Decreased levels of CDC25C were observed in SW480 cells treated with the combination of Eri plus LINSI for 24 h and in HCT116 cells treated with Eri alone for 24 h, consistent with G<sub>2</sub>/M



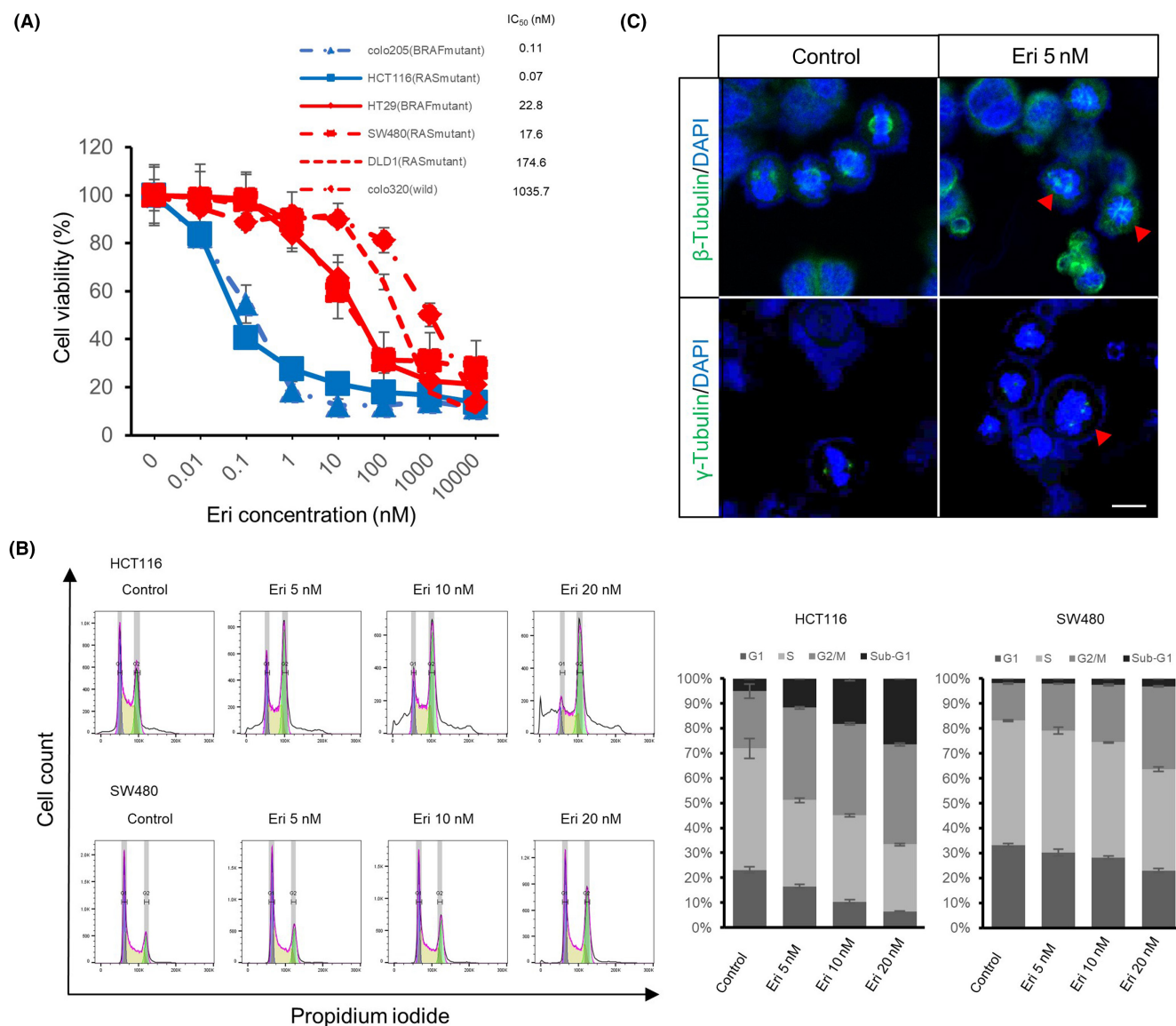
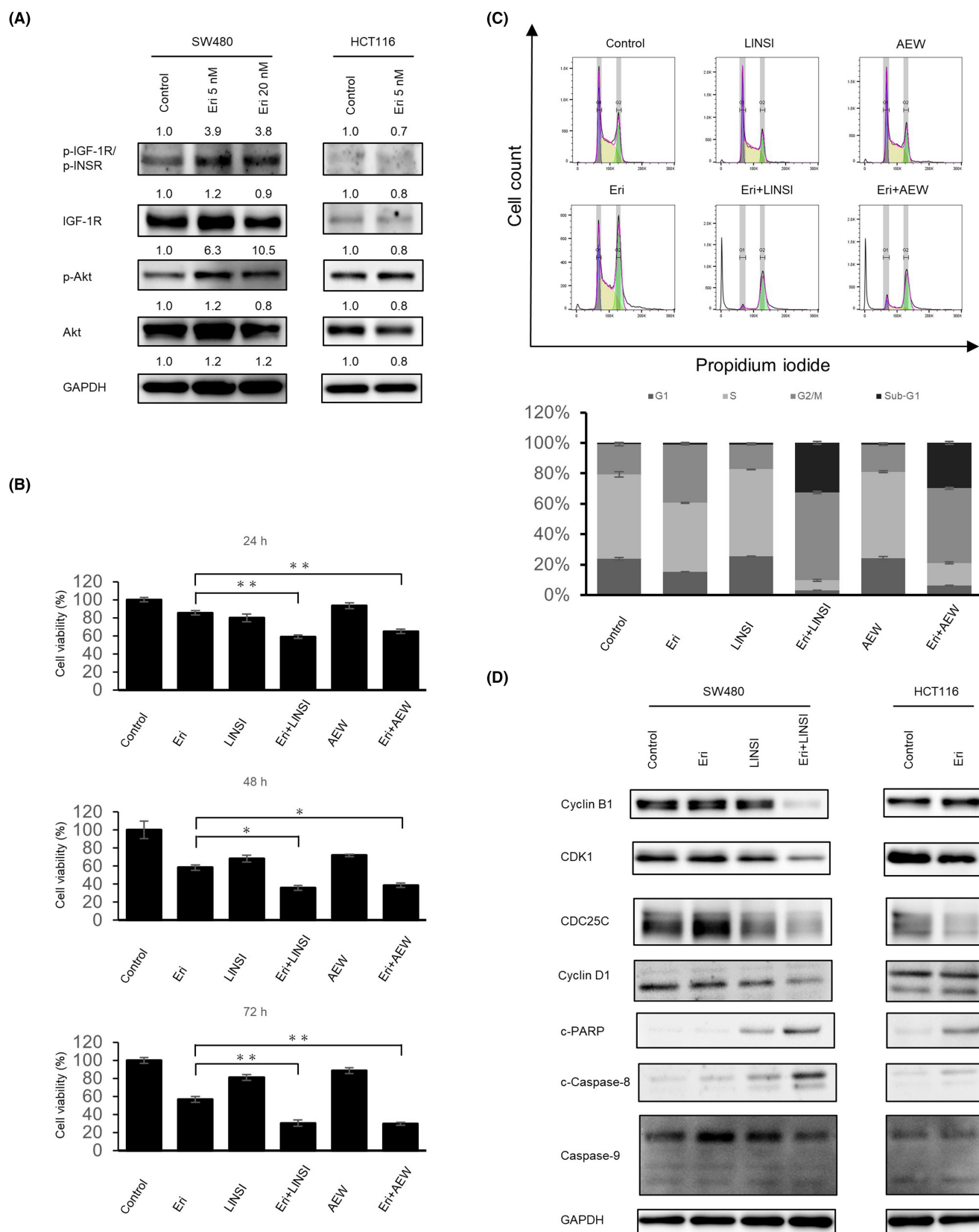


**FIGURE 1** Analysis of eribulin (Eri) sensitivity and mechanism of action in colorectal cancer (CRC) cell lines. (A) WST-8 assays were used to assess the viability of CRC cells after 72 h Eri exposure. Error bars represent SD of triplicate cultures. (B) Cell cycle analyses of HCT116 and SW480 cell lines exposed to the indicated concentrations of Eri for 24 h were undertaken by quantifying DNA content using flow cytometry. Cell cycle distribution is represented as mean  $\pm$  SD of triplicate cultures in the graph in the right panel. (C) Immunofluorescence image of HCT116 cells following treatment for 24 h with 5 nM Eri and staining for  $\beta$ -tubulin and  $\gamma$ -tubulin. The nucleus was counterstained with DAPI. Arrowheads indicate abnormal mitotic spindle structures. Scale bar, 10  $\mu$ m

**FIGURE 2** Activation of the insulin-like growth factor 1 receptor (IGF-1R)/insulin receptor (INSR) pathway confers eribulin (Eri) resistance. (A) SW480 and HCT116 cells were treated with the indicated concentrations of Eri for 72 h and then lysed and analyzed by western blotting. Relative protein levels were quantified using Fusion Solo 7 software. (B) Viability of SW480 cells measured by WST-8 assay following exposure to the indicated compounds for 24, 48, and 72 h. Concentrations of Eri, linsitinib (LINSI), and NVP-AEW541 (AEW) were 20 nM, 5  $\mu$ M, and 500 nM, respectively. Data are shown as mean  $\pm$  SD of triplicate cultures. \* $p$  < 0.001, \*\* $p$  < 0.0001, Tukey–Kramer tests. (C) Cell cycle analysis of SW480 cells following exposure to the indicated compounds. Cell cycle distribution is represented as mean  $\pm$  SD of triplicate cultures in the graph below. (D) Cell lysates of SW480 and HCT116 cells following exposure to the indicated compounds for 24 h were analyzed by western blotting. Eri concentrations were 20 and 5 nM for SW480 and HCT116 cells, respectively. LINSI and AEW concentrations were 5  $\mu$ M and 500 nM, respectively



phase arrest (Figure 2D). Although the levels of cleaved PARP, an apoptosis marker, were elevated both in combination therapy-treated SW480 and Eri-treated HCT116 cells, the levels of cyclin B1, cyclin D1, and CDK1 were decreased only in SW480 cells treated

with the combination of compounds, suggesting that a distinct mechanism of action underlies the response to combination therapy. To distinguish whether the mechanism of apoptosis is extrinsic or intrinsic, we analyzed caspase-8 and caspase-9 expression and found

that caspase-8, but not caspase-9, was activated by Eri and LINSI in combination, indicating that the apoptosis is exogenous.

### 3.3 | Activation of IGF-1R is responsible for Eri resistance

To further validate the results seen with the IGF-1R/INSR tyrosine kinase inhibitors, we established *IGF-1R* and *INSR* KO cell lines by mutating the genes using a CRISPR-Cas9 system. Specifically, two separate lines (KO1 and KO2) were established for knockouts of each gene, each using two different sgRNA sequences, for a total of four lines. Western blot analysis was used to confirm that the KO lines lacked expression of the respective receptor encoded by the gene targeted for disruption (Figure 3A).

Next, we examined the effect of *IGF-1R/INSR* KO on Eri efficacy by using the WST-8 assay. Although *IGF-1R* KO ameliorated Eri resistance in SW480 cells, *INSR* KO did not, suggesting that IGF-1R

is responsible for Eri resistance (Figure 3B). Cell cycle analysis also showed that Eri induced more profound G<sub>2</sub>/M arrest in *IGF-1R* KO cells (Figure 3C), yielding a pattern that resembled that seen for SW480 cells treated with the combination of Eri plus IGF-1R/INSR inhibitor.

These results showed that activation of IGF-1R confers Eri resistance, while disruption of the gene encoding IGF-1R enhances Eri efficacy by augmenting the effect of inducing G<sub>2</sub>/M arrest.

### 3.4 | Translocation of IGF-1R to the nucleus contributes to Eri resistance

Next, we investigated the mechanism whereby IGF-1R contributes to Eri resistance. Nuclear IGF-1R has been reported to accumulate to higher levels in CRC harboring mutations in *BRAF* than in CRC harboring mutations in *RAS* or CRC unmutated in *RAS* or *BRAF*, with nuclear IGF-1R protein levels correlating with chemotherapy

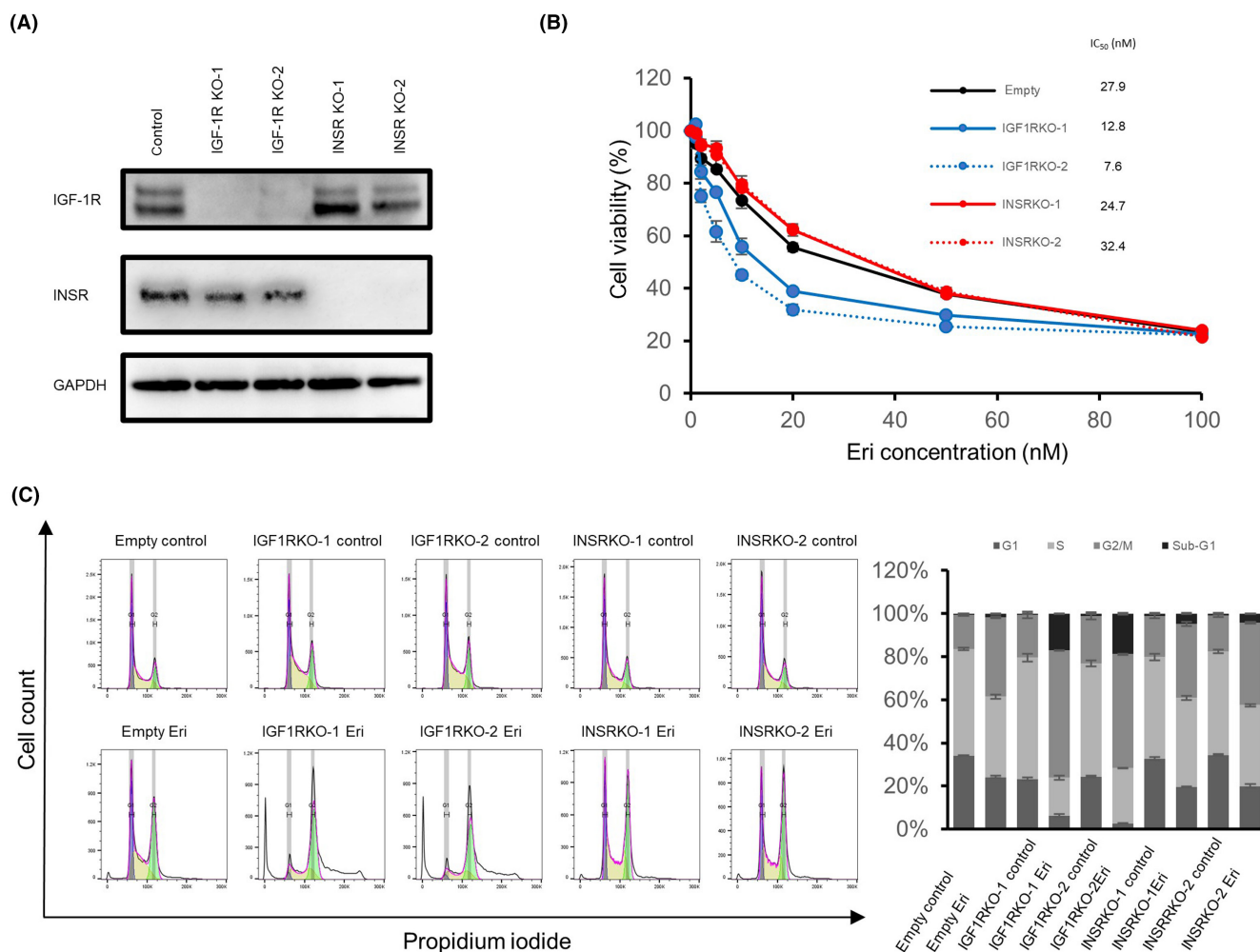


**FIGURE 3** Insulin-like growth factor-1 receptor (IGF-1R) activation is responsible for eribulin (Eri) resistance. (A) *IGF-1R* or insulin receptor (*INSR*) KO SW480 (generated using a CRISPR-Cas9 system) were lysed and analyzed by western blotting. (B) Empty vector-transduced and *IGF-1R* or *INSR* KO SW480 cells were exposed to the indicated concentrations of Eri for 72 h and then cell viability was measured by the WST-8 assay. Data are presented as mean ± SD of triplicate cultures. (C) Control SW480 and KO cells were exposed to 20 nM Eri for 24 h and then collected to analyze cell cycle. Cell cycle distribution is represented as mean ± SD of triplicate cultures in the graph to the right

resistance.<sup>17</sup> We hypothesized that nuclear IGF-1R participates in Eri resistance in CRC.

Immunofluorescent staining revealed nuclear translocation of IGF-1R in SW480 cells following exposure to Eri; however, nuclear translocation of IGF-1R was not observed when this cell line was exposed to the combination of LINSI and Eri (Figure 4A). Given that cell surface-located IGF-1R undergoes clathrin-dependent endocytosis and is translocated to the nucleus by importin  $\beta$ ,<sup>18</sup> we wondered whether inhibitors of endocytosis and importin  $\beta$  would also inhibit the Eri-induced nuclear translocation of IGF-1R. Indeed, as shown in Figure 4A, such inhibitors (chlorpromazine hydrochloride [CPZ] and importazole [IMPZ], respectively) impaired Eri-induced nuclear localization of IGF-1R.

To further confirm the contribution of nuclear IGF-1R to Eri resistance, the combined effects of Eri and CPZ or Eri and IMPZ were assessed. Both combinations potentiated Eri-induced G<sub>2</sub>/M arrest (Figure 4B) and inhibited cell proliferation more effectively than any of the compounds alone (Figure 4C).

Analysis of cell cycle and apoptosis-related protein levels by western blotting showed that Eri and CPZ or Eri and IMPZ provided changes similar to those seen with the combination of Eri plus LINSI (Figure 4D).

These results indicated that Eri-induced activation and subsequent nuclear translocation of IGF-1R correlates with Eri resistance.

### 3.5 | Combination of Eri and IGF-1R inhibitor induces ROS-mediated DNA damage

Given the potential benefit of combining Eri with IGF-1R inhibition, we next explored the underlying mechanism of the combined efficacy. Notably, previous reports indicated that the activation and nuclear localization of IGF-1R is necessary to repair DNA damage<sup>10</sup>; therefore, we investigated whether Eri exposure induces DNA damage when combined with IGF-1R inhibition, using immunofluorescent staining of  $\gamma$ H2AX, a marker of DNA damage. We observed increased  $\gamma$ H2AX staining in SW480 cells following exposure to the combination of Eri and LINSI compared to a control culture, indicating that the combination therapy induces DNA damage (Figure 5A).

Inhibition of microtubule polymerization could result in increased ROS production, leading in turn to DNA damage.<sup>19</sup> Therefore, we hypothesized that the combination of Eri plus LINSI enhances ROS production in Eri-resistant cell lines. We found that exposure of Eri-resistant SW480 cells to Eri or LINSI alone induced the production of a low level of ROS, but a larger increase was observed when the two compounds were combined (Figure 5B). In contrast, Eri-sensitive HCT116 cells showed no apparent increase compared to a control culture in the number of  $\gamma$ H2AX foci or ROS following exposure to the combination of Eri and LINSI, suggesting that a distinct mechanism of action is engaged by the combination Eri and LINSI in Eri-resistant cells.

To assess whether ROS-induced DNA damage contributes to G<sub>2</sub>/M arrest, we used N-acetyl-L-cysteine (NAC) as a ROS scavenger. As shown in Figure 5C, the induction of G<sub>2</sub>/M arrest and subsequent apoptosis seen in SW480 cells following exposure to the combination of Eri and LINSI was attenuated in the presence of NAC.

These findings indicated that the combination of Eri and LINSI induces ROS-mediated DNA damage and subsequent G<sub>2</sub>/M arrest, suggesting a new chemotherapeutic strategy for the use of Eri as an inducer of DNA damage.

### 3.6 | Combined Eri and LINSI inhibits tumor growth in vivo

Finally, we evaluated the in vivo antitumor activity of the combination of Eri and LINSI. Specifically, we implanted NSG mice subcutaneously with SW480 cells. In the absence of effective treatment, these mice developed subcutaneous tumors at the site of implantation. However, treatment of the tumor-implanted animals with the combination of Eri (0.25 mg/kg, i.v. once per week) and LINSI (50 mg/kg, by oral gavage once daily) led to attenuation of in-life tumor volume compared to control animals and to animals treated with Eri alone (Figure 6A). Similarly, tumor weights at necropsy were lower in mice treated with the combination of Eri and LINSI than in control animals and animals treated with Eri alone (Figure 6B). Although loss of 7% of bodyweight compared to baseline was seen in the combination-dosed mice, these animals subsequently recovered the lost bodyweight, indicating the feasibility of using the combination of Eri and LINSI for treatment of CRC (Figure 53). Immunohistochemical staining of tumor tissue for Ki-67 showed a decrease in the proportion of proliferating cells in animals treated with LINSI alone, and a further decrease in animals treated with the combination regimen (Figure 6C).

To assess whether IGF-1R was translocated to the nucleus following in vivo exposure to Eri, we undertook immunofluorescent staining of IGF-1R in tumor tissues recovered from tumor-implanted mice. As shown in Figure 6D, dosing of tumor-bearing mice with Eri alone induced nuclear translocation of IGF-1R, an effect that was counteracted by dosing with the combination of Eri and LINSI. This result indicated the significance of IGF-1R signaling for Eri resistance in vivo.

Taken together, these results suggested that inhibition of IGF1-R activity and/or translocation could overcome Eri resistance, offering a therapeutic opportunity in CRC.

## 4 | DISCUSSION

Most CRC shows a chromosomal instability (CIN) phenotype; pre-clinical study has shown that CIN confers taxane resistance.<sup>20</sup> Several clinical studies assessed the clinical activity of MTAs in patients with CRC by classifying these individuals using a putative



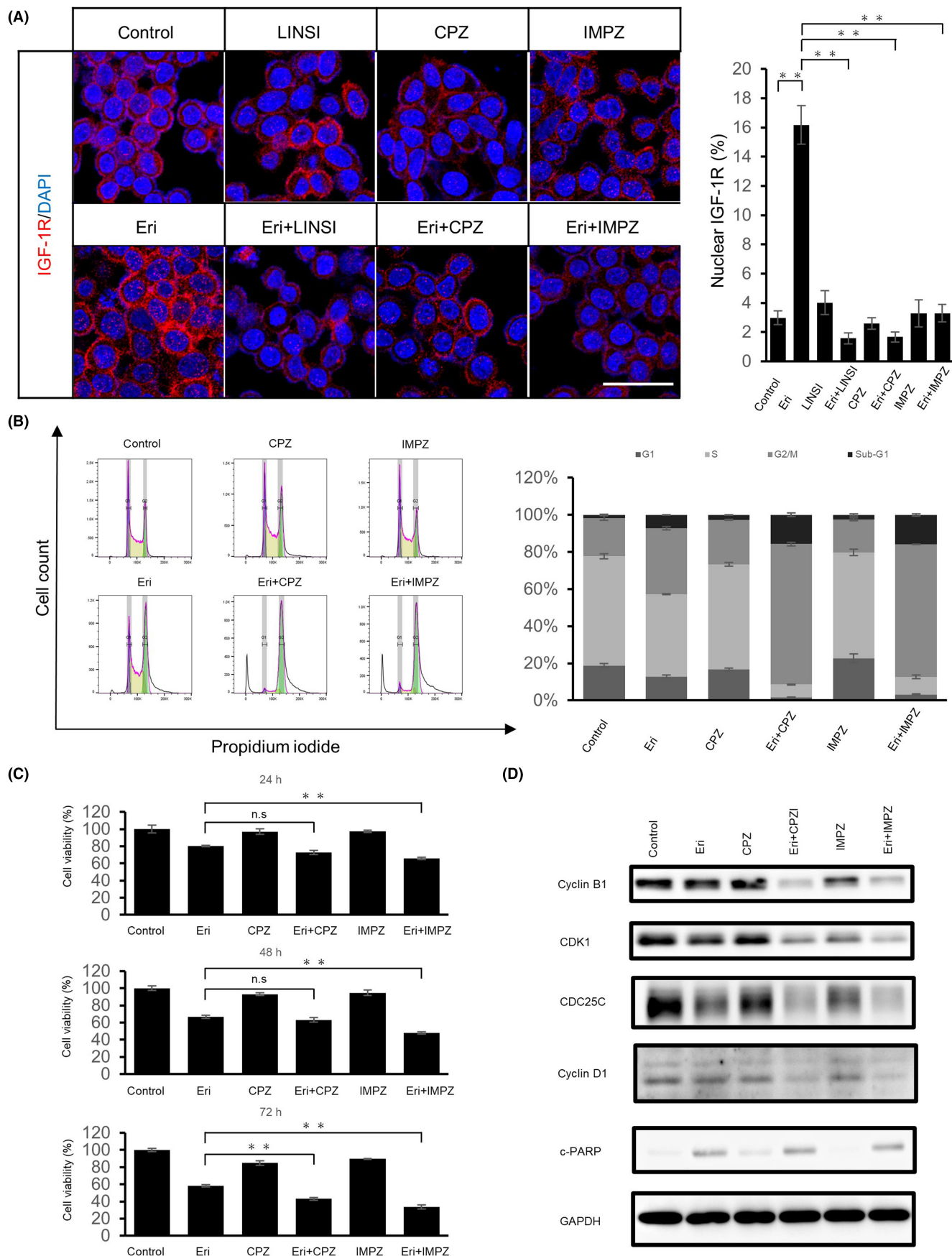


**FIGURE 4** Translocation of insulin-like growth factor-1 receptor (IGF-1R) to the nucleus contributes to eribulin (Eri) resistance. A, SW480 cells were exposed to the indicated compounds for 12 h and then subjected to immunofluorescent staining for IGF-1R. The nucleus was counterstained with DAPI. Scale bar, 50  $\mu$ m. The number of nuclear IGF-1R-positive cells as a percentage of total cells was quantified and mean  $\pm$  SD across five fields of view is shown in the graph to the right. \* $p$  < 0.001, \*\* $p$  < 0.0001, Tukey–Kramer tests. n.s, not significant. (B) Cell cycle of SW480 cells following exposure to the indicated compounds for 24 h was analyzed by flow cytometry. Cell cycle distribution is represented as mean  $\pm$  SD of triplicate cultures in the graph to the right. (C) Cell viability of SW480 cells measured by WST-8 assay following exposure to the indicated compounds for 24, 48, and 72 h. Data are shown as mean  $\pm$  SD of triplicate cultures. \* $p$  < 0.001, \*\* $p$  < 0.0001, Tukey–Kramer tests. n.s, not significant. (D) Cell lysates of SW480 cells following exposure to the indicated compounds for 24 h were analyzed by western blotting. CPZ, chlorpromazine hydrochloride; IMPZ, importazole; LINSI, linsitinib

predictive biomarker, but all such studies failed to show efficacy of MTAs,<sup>3,4,21</sup> indicating the challenge of identifying predictive biomarkers for the use of MTAs in CRC. In the present study, we showed that the combination of Eri and LINSI, an IGF-1R inhibitor, restored activity against Eri-resistant CRC cells; we further demonstrated that nuclear translocation of IGF-1R led to phosphorylation of the protein, contributing to Eri resistance.

Two of six tested CRC cell lines were sensitive to Eri, showing subnanomolar IC<sub>50</sub> values; however, the majority of the tested cell lines were resistant to Eri, which permitted us to explore the mechanism of resistance. Resistant cells showed activation of IGF-1R signaling after Eri exposure, whereas incubation with an IGF-1R inhibitor sensitized such cell lines to Eri, a pattern similar to that seen in ovarian cancer exposed to paclitaxel, another MTA.<sup>7</sup> Although that report showed that *IGF2* mRNA (encoding insulin-like growth factor 2) accumulated following exposure to paclitaxel and that IGF-2 modulated resistance to this compound, no known agonist of IGF-1R was significantly upregulated at the mRNA level by Eri in our experiment (data not shown). Therefore, we utilized a CRISPR-Cas9 system to mutate the *IGF-1R* gene and confirm the contribution of IGF-1R to Eri resistance. Knockout experiments confirmed that IGF-1R modulates Eri resistance and indicated that Eri resistance might involve a mechanism of action distinct from the well-known agonist-mediated one. For example, cross-talk with other RTKs could affect and activate IGF-1R signaling following Eri exposure. Clearly, further study will be needed to elucidate the mechanism of IGF-1R activation following Eri exposure.

Regarding the proposed strategy of combining IGF-1R signaling inhibition with MTAs, a recent phase III clinical trial in patients with advanced non-small-cell lung cancer failed to show efficacy for the combination of figitumumab, an Ab specifically directed against IGF-1R, with carboplatin and paclitaxel.<sup>22</sup> Phosphorylation of IGF-1R is necessary for nuclear translocation of IGF-1R by importin  $\beta$  (8.18). Although LINSI inhibited Eri-induced nuclear translocation of IGF-1R in the present work, a previous report showed that the monoclonal anti-IGF-1R Ab ganitumab increased the nuclear translocation of IGF-1R.<sup>17</sup> Clinical failure of the combination of paclitaxel and an anti-IGF-1R Ab could be explained in part by a failure to inhibit nuclear translocation of IGF-1R; thus, an IGF-1R tyrosine kinase inhibitor might be a better partner for combining with an MTA.

Microtubule targeting agents are known to induce mitotic arrest by suppressing microtubule dynamics.<sup>23</sup> In the present work,

Eri-sensitive CRC cells underwent mitotic arrest following exposure to Eri, but resistant cells were not subject to mitotic arrest, and the accompanying nuclear translocation of IGF-1R facilitated the repair of DNA damage. Although mitotic arrested Eri sensitive cells undergo apoptosis without DNA damage, resistant cells undergo apoptosis only after DNA damage by Eri and LINSI in combination. Therefore, we infer that when the mitotic arrest-inducing effect of Eri is insufficient to kill cells, the potent function of Eri as a DNA-damaging agent is revealed by inhibiting the activity and/or nuclear translocation of IGF-1R.

Microtubule targeting agents such as paclitaxel and vincristine promote ROS generation through generation of extracellular H<sub>2</sub>O<sub>2</sub> from the membrane-associated NADPH oxidase, a process referred to as a toxic bystander effect, and is distinct from the induction of mitotic arrest.<sup>19</sup> Regarding IGF-1R signaling, the metformin derivative HL156A has been shown to inhibit the activation of IGF-1R, thereby inducing apoptotic cell death through ROS production.<sup>24</sup> Hyperphosphorylation of Aurora A is induced by ROS, leading in turn to significant mitotic delays due to abnormal mitotic spindle assembly.<sup>25</sup> Taken together, these results suggest that the combination of Eri and an IGF-1R inhibitor could synergistically enhance ROS production, inducing DNA damage and subsequent G<sub>2</sub>/M arrest.

Reactive oxygen species was reported to induce apoptosis through extrinsic or intrinsic pathways.<sup>26</sup> In our study, cleaved caspase-8 was detected after the treatment of Eri and LINSI combination, suggesting an extrinsic pathway was involved. In fact, FAS and FAS ligand were upregulated in murine intestinal epithelial cells after H<sub>2</sub>O<sub>2</sub> treatment,<sup>27</sup> and NHL-repeat-containing protein 2 (NHLRC2) cleaved by caspase-8 was involved in ROS-induced apoptosis in HCT116 human CRC cells.<sup>28</sup> However, the precise downstream mechanism of caspase-8 activation remains elusive.

One of the limitations of our study was that all experiments were undertaken using CRC cell lines; clinical specimens were not assessed, given that Eri or other MTAs have not been used for the treatment of CRC in clinical settings. The nuclear localization of IGF-1R might serve as a marker for identifying the presence of a *BRAF* mutation in CRC and predict chemotherapy resistance.<sup>17</sup> Our results could explain the failure of using *BRAF* mutational status as a predictive biomarker of sensitivity to Eri and vinorelbine, as nuclear IGF-1R, which is more frequently expressed in *BRAF* mutant patients, could contribute in part to MTA resistance.

In summary, we showed that the combination of Eri and LINSI was effective against CRC, both in vitro and in vivo. These results

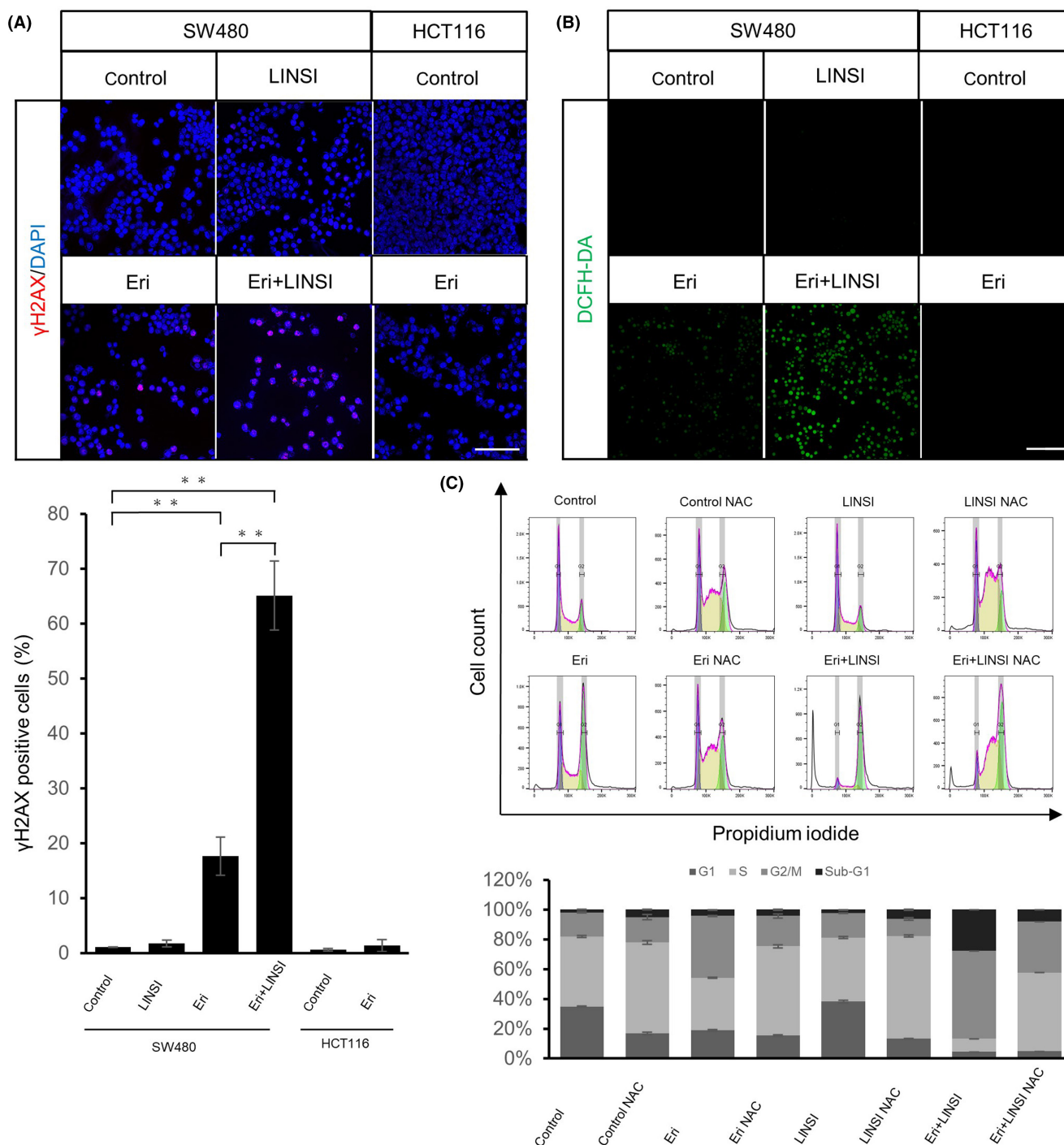


**FIGURE 5** Combination of eribulin (Eri) and insulin-like growth factor-1 receptor (IGF-1R) inhibitor induces reactive oxygen species (ROS)-mediated DNA damage. (A) SW480 and HCT116 cells were exposed to the indicated compounds for 24 h and then subjected to immunofluorescent staining for  $\gamma$ H2AX. The number of  $\gamma$ H2AX-positive cells as a percentage of total cells was quantified. Mean  $\pm$  SD of three fields is shown in the graph below.  $**p < 0.0001$ , Tukey–Kramer tests. Scale bar, 50  $\mu$ m. B, SW480 and HCT116 cells were exposed to the indicated compounds for 24 h and then stained with dichloro-dihydro-fluorescein diacetate (DCFH-DA). Scale bar, 100  $\mu$ m. (C) Cell cycle analysis of SW480 cells following exposure to the indicated compounds for 24 h. N-acetyl-L-cysteine (NAC) (5 mM), used as a ROS scavenger, was added starting 1 h before initiation of exposure to the indicated compounds. Cell cycle distribution is represented as mean  $\pm$  SD of triplicate cultures in the graph below. LINSI, linsitinib

provide a proof of concept for the potential use of the combination of Eri and an IGF-1R inhibitor for the clinical treatment of patients with CRC. Our study also suggested a mechanism of action for this

combination, suggesting that Eri plus LINSI could provide efficacy by inducing ROS-mediated DNA damage, implying a mechanism of action distinct from that seen with MTAs alone.



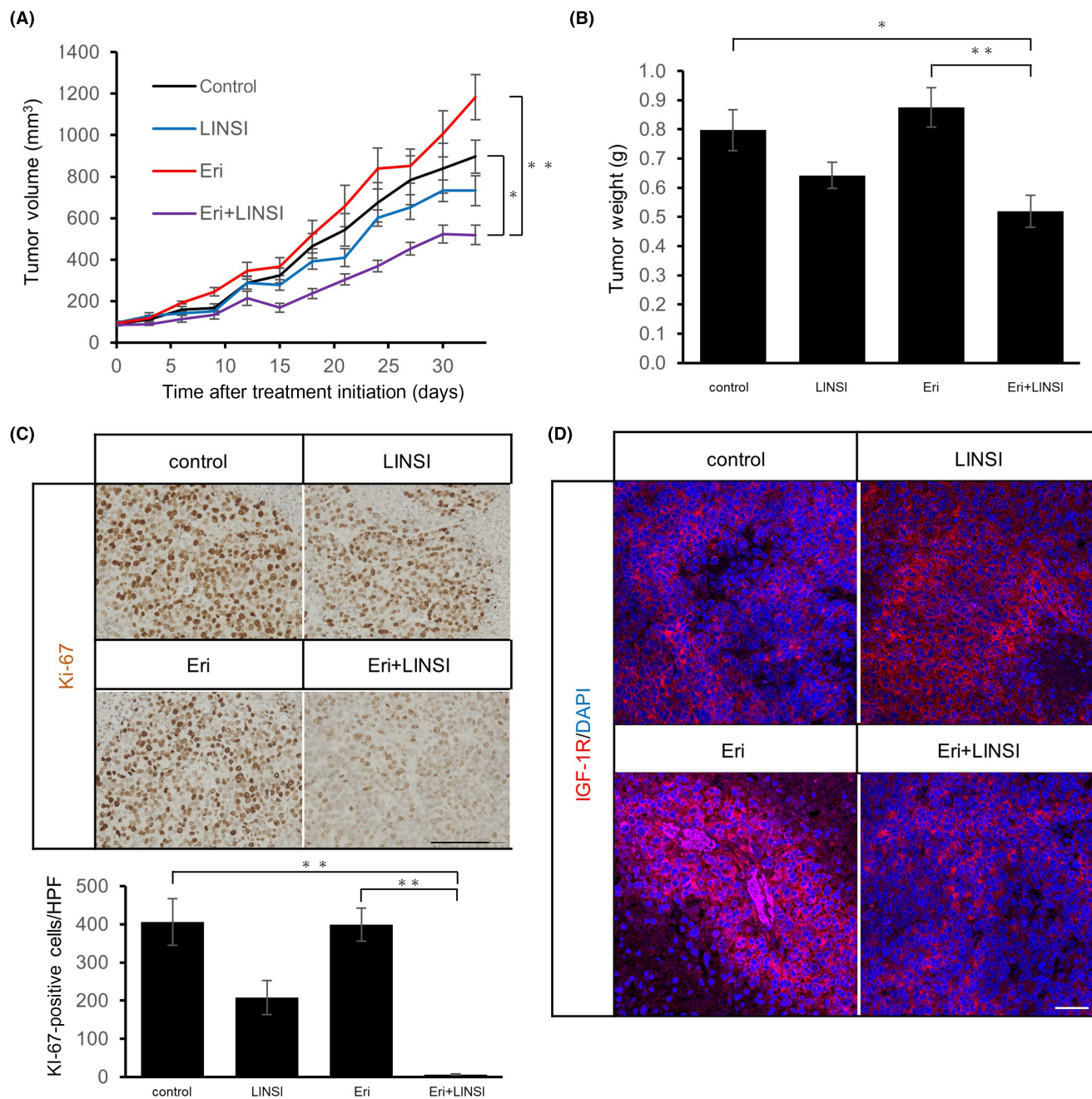


**FIGURE 6** Combination of eribulin (Eri) and linsitinib (LINSI) attenuates tumor growth in vivo. (A) SW480 cells were implanted into NSG mice. Tumor-bearing mice were then treated with vehicle ( $n = 8$ ), 50 mg/kg LINSI ( $n = 8$ ), 0.25 mg/kg Eri ( $n = 8$ ), or the combination of Eri plus LINSI ( $n = 7$ ). Eri was given intravenously once per week; LINSI was given once daily by oral gavage. Mean  $\pm$  SEM of the calculated in-life tumor volumes are shown.  $*p < 0.05$ ,  $**p < 0.0001$ , Tukey–Kramer tests. (B) Terminal tumor weights of xenografted tumors are shown as mean  $\pm$  SEM.  $*p < 0.05$ ,  $**p < 0.01$ , Tukey–Kramer tests. (C) Image of immunohistochemical staining of xenografted tumor using anti-Ki-67 Ab. Number of Ki-67-positive cells per high-power field (HPF) was counted; mean  $\pm$  SD of 12 HPF/tumor is shown in the graph below.  $**p < 0.0001$ , Tukey–Kramer tests. Scale bar, 100  $\mu$ m. (D) Immunofluorescent staining for insulin-like growth factor-1 receptor (IGF-1R) using serial sections of samples from (C). Nucleus was counterstained with DAPI. Scale bar, 50  $\mu$ m

## ACKNOWLEDGMENT

We thank Hiroshi Fujii for providing pathological specimens. This work was supported by the Shinnihon Foundation of Advanced Medical Treatment Research.

## DISCLOSURE

Koichi Akashi is an Editorial Board Member of *Cancer Science* and received scholarship endowment from Eisai Corporation. The other authors have no conflict of interest.

## ETHICS STATEMENT

Approval of the research protocol by an Institutional Review Board: N/A.

Informed consent: N/A.

Registry and registration no. of the study/trial: N/A.

Animal studies: The animal study protocol was approved by the Ethics Committee of Kyushu University (Approval No. A-21-227-0).

## ORCID

Hiroshi Ariyama  <https://orcid.org/0000-0002-8374-5045>

Taichi Isobe  <https://orcid.org/0000-0001-5686-1940>

Eishi Baba  <https://orcid.org/0000-0001-9428-6772>

## REFERENCES

- WHO cancer today (2018). Accessed February 1, 2022. <https://gco.iarc.fr/today/home>
- Vecchione L, Gambino V, Raaijmakers J, et al. A vulnerability of a subset of colon cancers with potential clinical utility. *Cell*. 2016;165(2):317-330.
- Cremolini C, Pietrantonio F, Tomasello G, et al. Vinorelbine in BRAF V600E mutated metastatic colorectal cancer: a prospective multicentre phase II clinical study. *ESMO Open*. 2017;2(3):e000241.
- Masuishi T, Taniguchi H, Kotani D, et al. A multicenter phase II study of eribulin in patients with BRAF V600E mutant metastatic colorectal cancer: BRAVERY study (EPOC1701). *Ann Oncol*. 2020;31(SUPPLEMENT3):S226. doi:10.1016/j.annonc.2020.04.040
- Pollak M. Insulin and insulin-like growth factor signalling in neoplasia. *Nat Rev Cancer*. 2008;8(12):915-928.
- Ireland L, Santos A, Campbell F, et al. Blockade of insulin-like growth factors increases efficacy of paclitaxel in metastatic breast cancer. *Oncogene*. 2018;37(15):2022-2036.
- Huang GS, Brouwer-Visser J, Ramirez MJ, et al. Insulin-like growth factor 2 expression modulates Taxol resistance and is a candidate biomarker for reduced disease-free survival in ovarian cancer. *Clin Cancer Res*. 2010;16(11):2999-3010.
- Aleksic T, Chitnis MM, Perestenko OV, et al. Type 1 insulin-like growth factor receptor translocates to the nucleus of human tumor cells. *Cancer Res*. 2010;70(16):6412-6419.
- Warsito D, Sjöström S, Andersson S, Larsson O, Sehat B. Nuclear IGF1R is a transcriptional co-activator of LEF1/TCF. *EMBO Rep*. 2012;13(3):244-250.
- Waraky A, Lin Y, Warsito D, Haglund F, Aleem E, Larsson O. Nuclear insulin-like growth factor 1 receptor phosphorylates proliferating cell nuclear antigen and rescues stalled replication forks after DNA damage. *J Biol Chem*. 2017;292(44):18227-18239.
- Guerard M, Robin T, Perron P, et al. Nuclear translocation of IGF1R by intracellular amphiregulin contributes to the resistance of lung tumour cells to EGFR-TKI. *Cancer Lett*. 2018;420:146-155.
- Bouwman P, Jonkers J. The effects of deregulated DNA damage signalling on cancer chemotherapy response and resistance. *Nat Rev Cancer*. 2012;12(9):587-598.
- Hao X, Wenqing B, Lv G, et al. Disrupted mitochondrial homeostasis coupled with mitotic arrest generates antineoplastic oxidative stress. *Oncogene*. 2022;41(3):427-443.
- Brian Dalton W, Nandan MO, Moore RT, Yang VW. Human cancer cells commonly acquire DNA damage during mitotic arrest. *Cancer Res*. 2007;67(24):11487-11492.
- Sanjana NE, Shalem O, Zhang F. Improved vectors and genome-wide libraries for CRISPR screening. *Nat Methods*. 2014;11(8):783-784.
- Reya T, Duncan AW, Ailles L, et al. A role for Wnt signalling in self-renewal of haematopoietic stem cells. *Nature*. 2003;423(6938):409-414.
- Codony-Servat J, Cuatrecasas M, Asensio E, et al. Nuclear IGF-1R predicts chemotherapy and targeted therapy resistance in metastatic colorectal cancer. *Br J Cancer*. 2017;117(12):1777-1786.
- Packham S, Warsito D, Lin Y, et al. Nuclear translocation of IGF-1R via p150(glued) and an importin- $\beta$ /RanBP2-dependent pathway in cancer cells. *Oncogene*. 2015;34(17):2227-2238.
- Alexandre J, Yumin H, Weiqin L, Pelicano H, Huang P. Novel action of paclitaxel against cancer cells: bystander effect mediated by reactive oxygen species. *Cancer Res*. 2007;67(8):3512-3517.
- Swanton C, Nicke B, Schuett M, et al. Chromosomal instability determines taxane response. *Proc Natl Acad Sci U S A*. 2009;106(21):8671-8676.
- Overman MJ, Adam L, Raghav K, et al. Phase II study of nab-paclitaxel in refractory small bowel adenocarcinoma and CpG Island methylator phenotype (CIMP)-high colorectal cancer. *Ann Oncol*. 2018;29(1):139-144.
- Langer CJ, Novello S, Park K, et al. Randomized, phase III trial of first-line figitumumab in combination with paclitaxel and carboplatin versus paclitaxel and carboplatin alone in patients with advanced non-small-cell lung cancer. *J Clin Oncol*. 2014;32(19):2059-2066.
- Steinmetz MO, Prota AE. Microtubule-targeting agents: strategies to hijack the cytoskeleton. *Trends Cell Biol*. 2018;28(10):776-792.
- Lam TG, Jeong YS, Kim S-A, Ahn S-G. New metformin derivative HL156A prevents oral cancer progression by inhibiting the insulin-like growth factor/AKT/mammalian target of rapamycin pathways. *Cancer Sci*. 2018;109(3):699-709.
- Wang G-F, Dong Q, Bai Y, et al. Oxidative stress induces mitotic arrest by inhibiting Aurora A-involved mitotic spindle formation. *Free Radic Biol Med*. 2017;103:177-187.
- Alonso MM, Asumendi A, Villar J, et al. New benzo(b)thiophene-sulphonamide 1,1-dioxide derivatives induce a reactive oxygen species-mediated process of apoptosis in tumour cells. *Oncogene*. 2003;22(24):3759-3769.
- Denning TL, Takaishi H, Crowe SE, Boldogh I, Jevnikar A, Ernst PB. Oxidative stress induces the expression of Fas and Fas ligand and apoptosis in murine intestinal epithelial cells. *Free Radic Biol Med*. 2002;33(12):1641-1650.
- Nishi K, Iwaihara Y, Tsunoda T. ROS-induced cleavage of NHLRC2 by caspase-8 leads to apoptotic cell death in the HCT116 human colon cancer cell line. *Cell Death Dis*. 2017;8(12):3218.

## SUPPORTING INFORMATION

Additional supporting information can be found online in the Supporting Information section at the end of this article.

**How to cite this article:** Yoshihiro T, Ariyama H, Yamaguchi K, et al. Inhibition of insulin-like growth factor-1 receptor enhances eribulin-induced DNA damage in colorectal cancer. *Cancer Sci*. 2022;113:4207-4218. doi: [10.1111/cas.15558](https://doi.org/10.1111/cas.15558)